Observed Structure and Characteristics of Cold Pools over Tropical Oceans using Scatterometer Vector Wind Retrievals

Piyush Garg[1], Stephen W. Nesbitt[1], Timothy J. Lang[2], Themis Chronis[3], Jeffrey D. Thayer[1], Deanna A. Hence[1]

[1] University of Illinois Urbana Champaign
[2] NASA Marshall Space Flight Center, Alabama
[3] University of Alabama Huntsville

Background

- Cold pool activity can significantly impact horizontal wind velocities at 10-30 km grid scale, leading to significant **inhomogeneity in surface fluxes** and trigger, organize, and suppress convection. (Tompkins 2001; Ross et al. 2004; Zuidema et al. 2012).

- To explore the connections between oceanic convection and cold pools, Elsaesser et al. (2013) used the QuikSCAT data over tropical oceans to calculate **cold pool kinetic energy (CPKE).**

- CPKE used observed QuikSCAT wind anomalies and their variance in surface winds over tropical oceans, and was hypothesized to be related to **cold pool outflow or mesoscale downdrafts** from nearby regions of convection.

- Elsaesser et al. (2013) did not consider rain contamination and assumed that CPKE was capturing wind variations around the rainfall maximum.

- Kilpatrick et al. (2015) used ASCAT data after removing rain contamination to observe MCS-related divergence. They found that ASCAT cannot detect convective-scale gust fronts, but can detect mesoscale downdrafts corresponding to cold pools.

- **Here, we propose and evaluate a new method that objectively identifies regions of cold pools using wind gradients.**

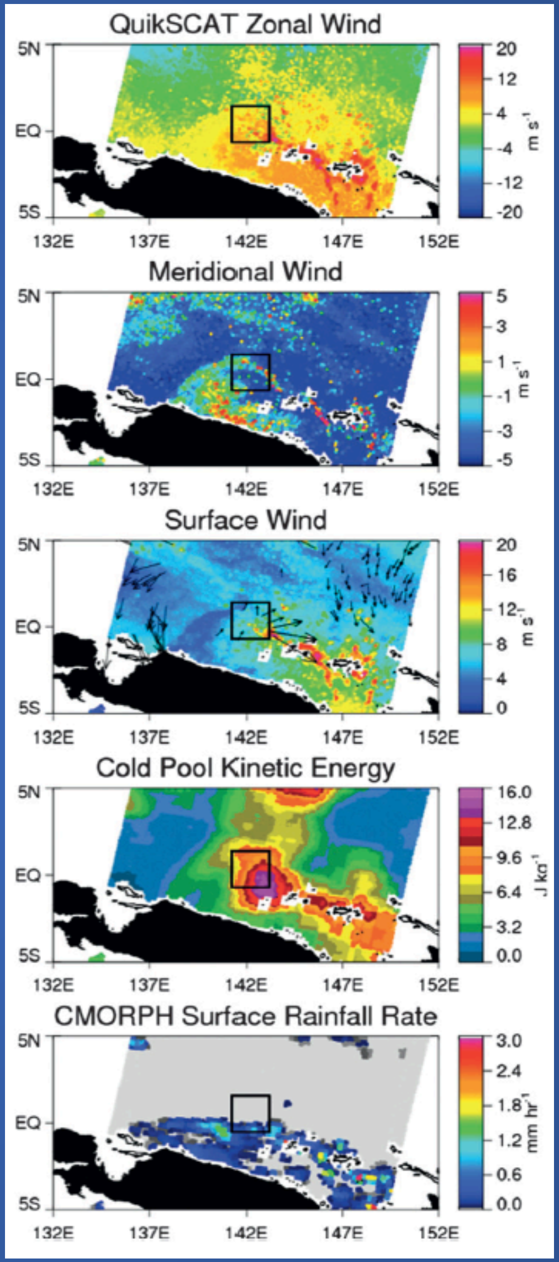

Elsaesser et al. (2013)

Motivation and Goals

- We hypothesize that an approach based on closed areas of wind gradients (or gradient features – GFs) can be used to identify the cold pools over tropical oceans.
- Cold pools form a gust front boundary, thus creating an area of steep gradients in horizontal winds.
- We identify the areas of increased scalar gradients in the horizontal wind using:

$$|\nabla \vec{V}| = \begin{bmatrix} \dfrac{\partial u}{\partial x} + \dfrac{\partial v}{\partial x} \\ \dfrac{\partial u}{\partial y} + \dfrac{\partial v}{\partial y} \end{bmatrix}$$

- After calculating gradient in the scatterometer winds, python's scikit-image convex hull algorithm (which encloses regions) was implemented to identify the perimeters of the GFs when the gradient exceeds 10^{-4} s^{-1}, and Sobel technique was used for edge detection.

GF identification using convex hull algorithm and Sobel technique

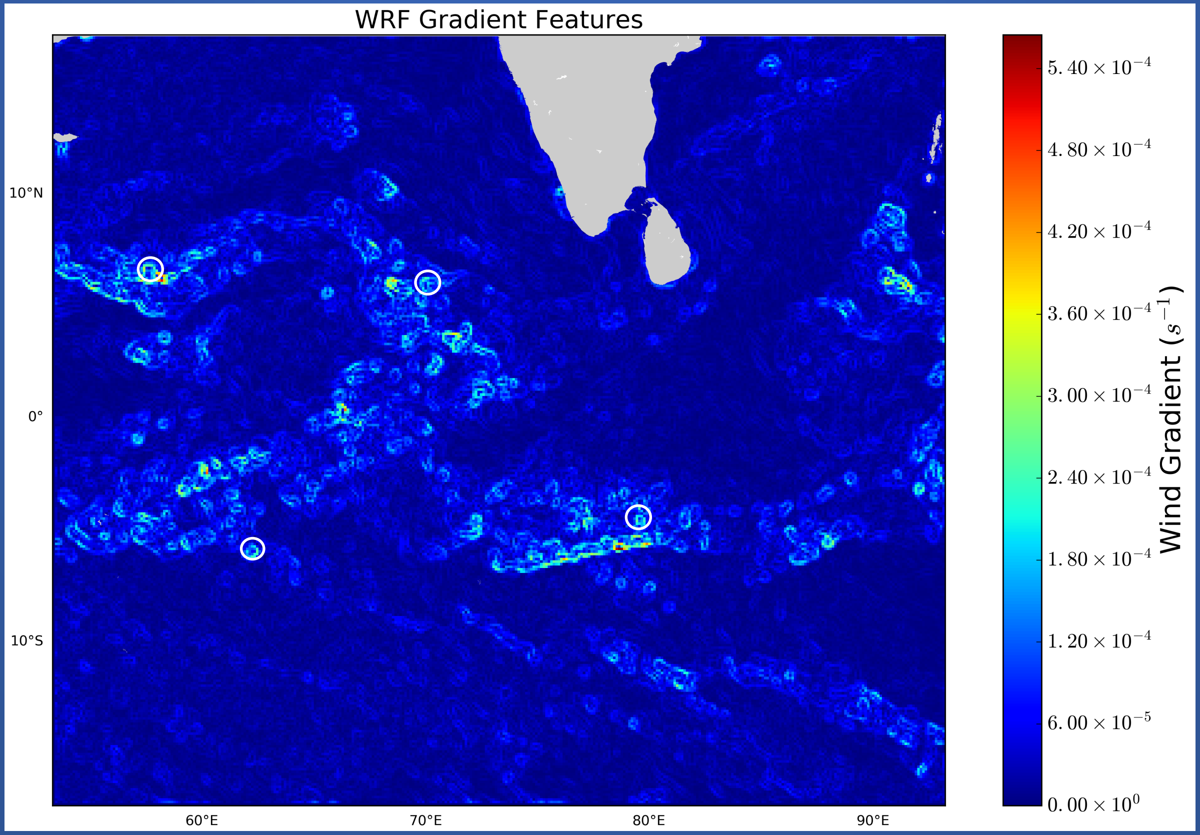

- Properties of individual GFs such as eccentricity, area, weighted centroid, etc. were calculated using scikit-image.

- Traditional kinematic diagnostics were performed surrounding each GF, including divergence $(\nabla . \vec{V})$ and vorticity $(\nabla \times \vec{V})$.

- In addition to a climatological analysis, to test our technique, GFs were obtained using WRF-simulated cold pools, winds and thermodynamic conditions.

Data used in this study

Global Observations

- ASCAT MetOp-A dataset from Remote Sensing Systems (REMSS) is used at 12.5 km resolution for the period of 2007-2015.

- The REMSS ASCAT dataset uses radiometer data to determine if rain is present within 3 hours at the location of ASCAT observation, in addition to scatterometer rain flag.

- CPC Morphing Technique (CMORPH) precipitation dataset for the above period at 8 km and 30-min resolution is used.

- Modern-Era Retrospective analysis for Research and Applications (MERRA-2) products were used to identify background fields.

Modeling Framework for evaluation of the GF technique

- WRF-ARW v3.8.1 was run on a nested grid of 27-9-3 km using initial conditions from GFS for 2 days during the active phase of DYNAMO MJO-1 with following schemes:

Physics	Parameterization Scheme
Simulation dates	**19 Oct 00Z - 21 Oct 00Z 2011**
Longwave Radiation	RRTMG
Shortwave Radiation	RRTMG
Microphysics	Thompson
Boundary Layer	YSU
Surface	Noah LSM
Cumulus	Tiedtke (27km and 9km)

- Convection was explicitly resolved in the 3-km domain, which produces cold pools that are observed to be similar to those observed during DYNAMO MJO-2 (Feng et al. 2015).

Evaluation Methodology

- WRF's 3-km grid was regridded to a 0.125° lat-lon grid using a weighting function similar to the ASCAT footprint, and GFs were calculated for the domain.

- To study the thermodynamic structure of WRF GFs, virtual temperature (T_v) was calculated from model parameters and WRF GFs were overlaid on T_v to see whether they collocate or not.

- Surface sensible and latent heat fluxes were calculated using MERRA-2 background field products and ASCAT winds, and compared to MERRA-2 fields.

- Precipitation from CMORPH was collocated with the gradient features within 8 degrees of the centroid of GF.

Gradient Features on 19-20 October 2011

WRF GFs

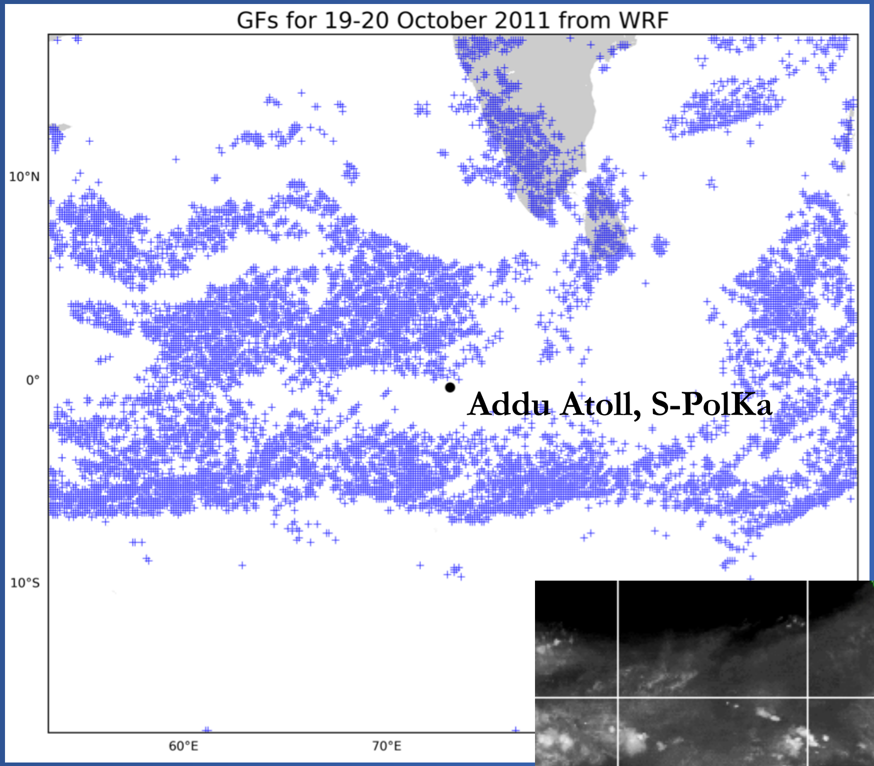

ASCAT GFs

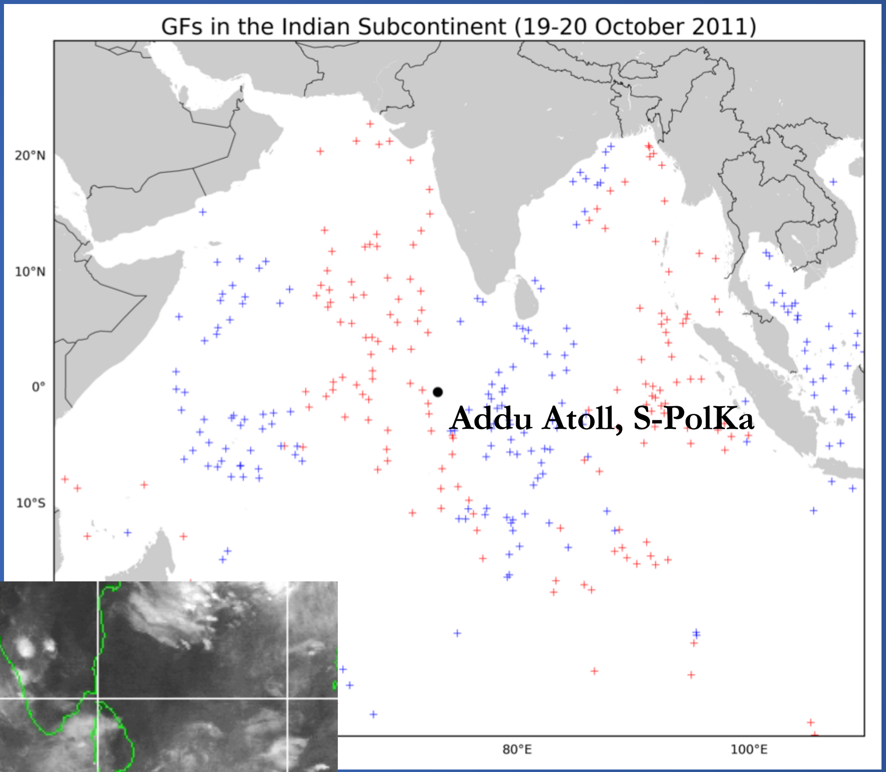

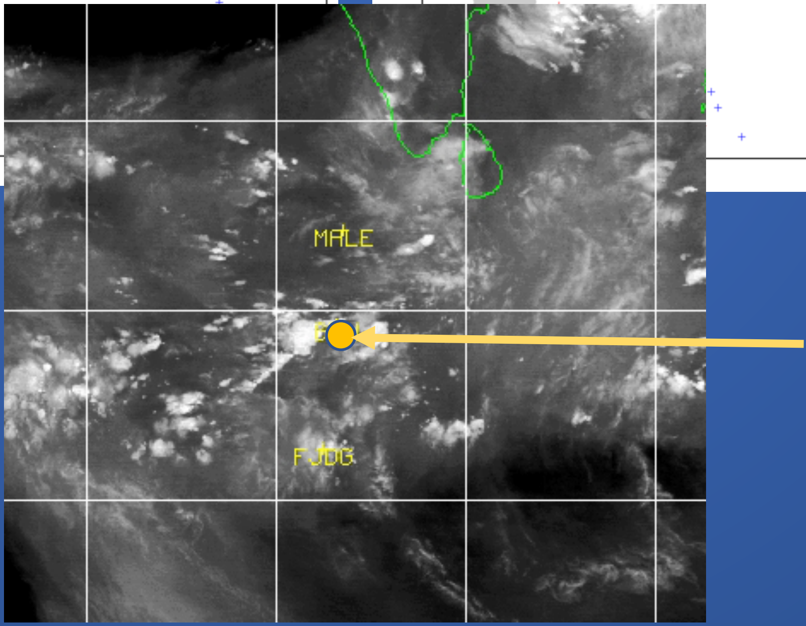

Meteosat-7 WV Imagery
1630 UTC 20 October 2011

Divergence and Vorticity for ASCAT (left) and MERRA-2 (right)

20 October 2011 16:32:17 UTC

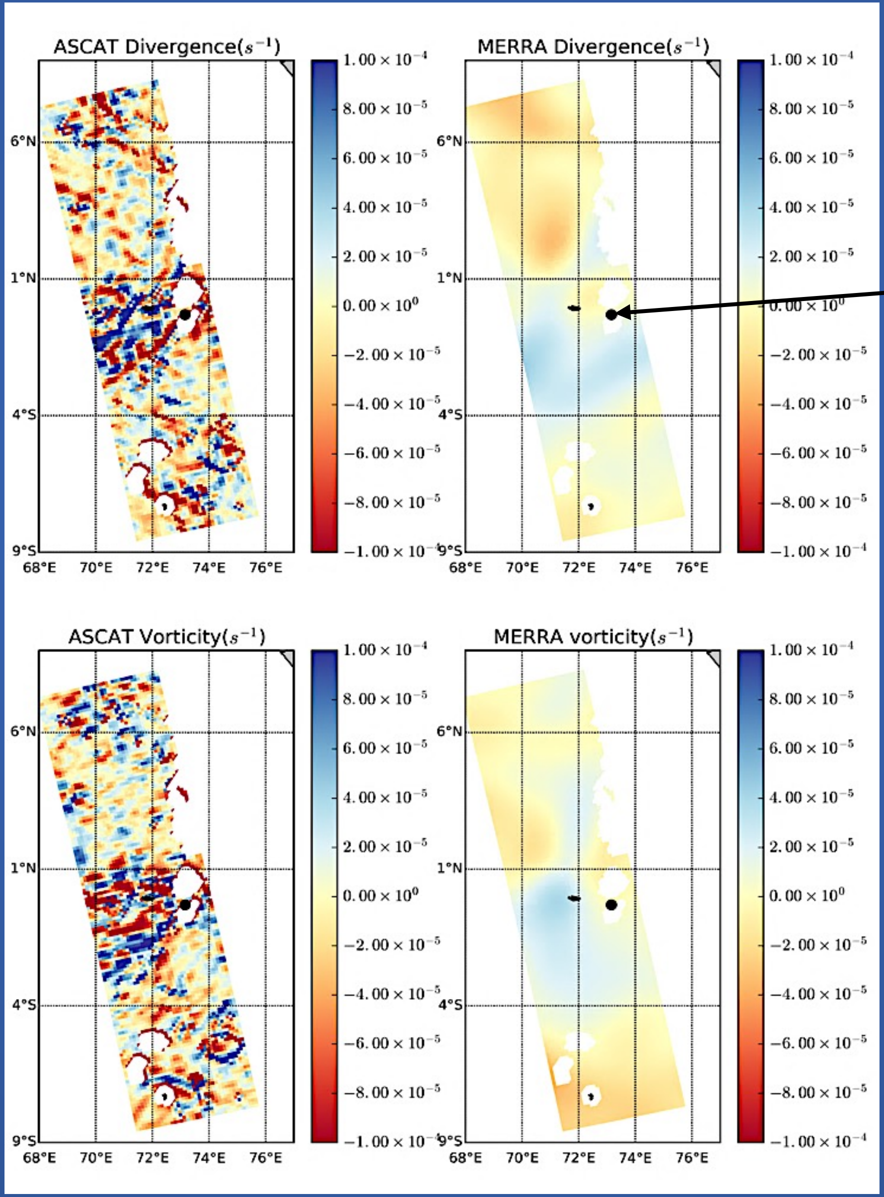

Addu Atoll, S-PolKa

Surface Latent heat and sensible heat flux (Wm^{-2}) and CMORPH precipitation (mm/hr)

20 October 2011 16:32:17 UTC

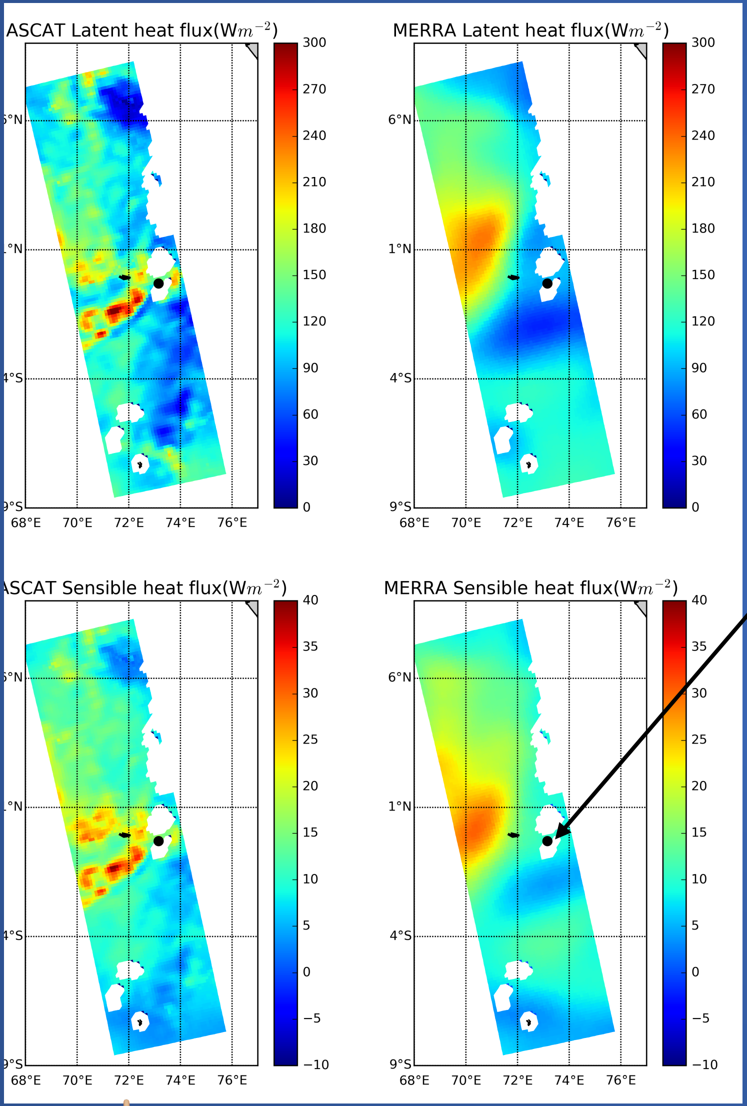

20 October 2011 16:30:00 UTC

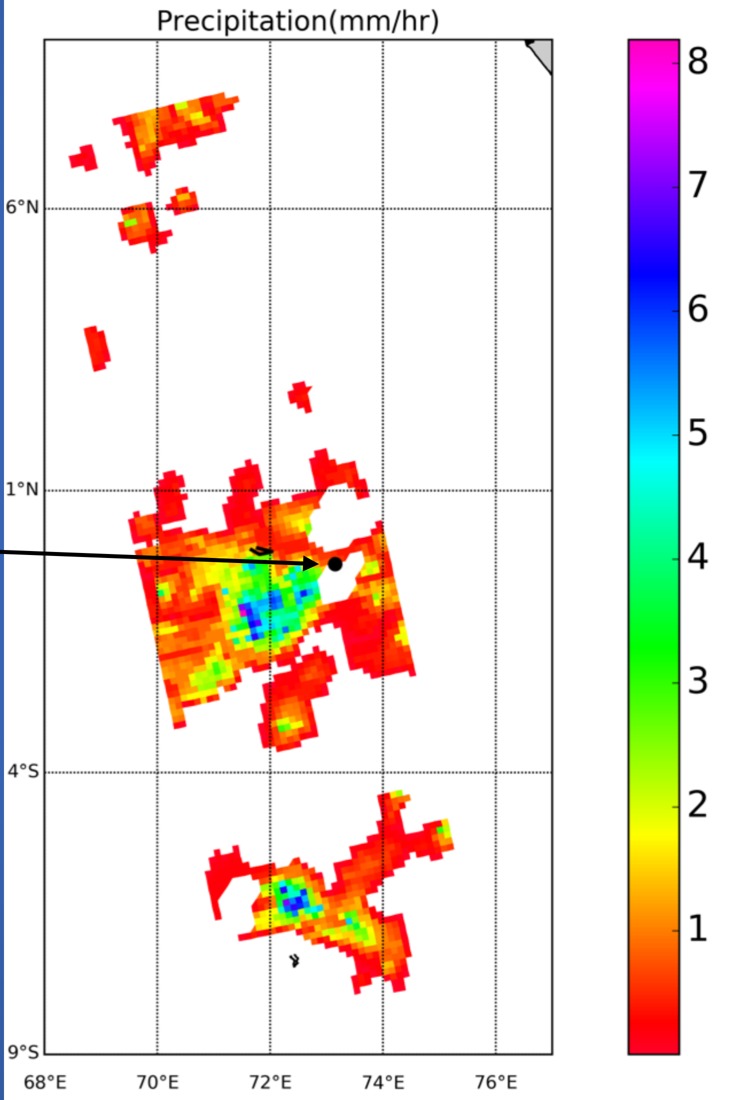

Addu Atoll, S-PolKa

👆 Replaced MERRA winds with ASCAT winds

NCAR S-PolKa radar

Reflectivity (dBZ) and Relative velocity (ms^{-1}) for 20 October 2011 16:32:21 UTC as measured from Addu Atoll during DYNAMO (2011)

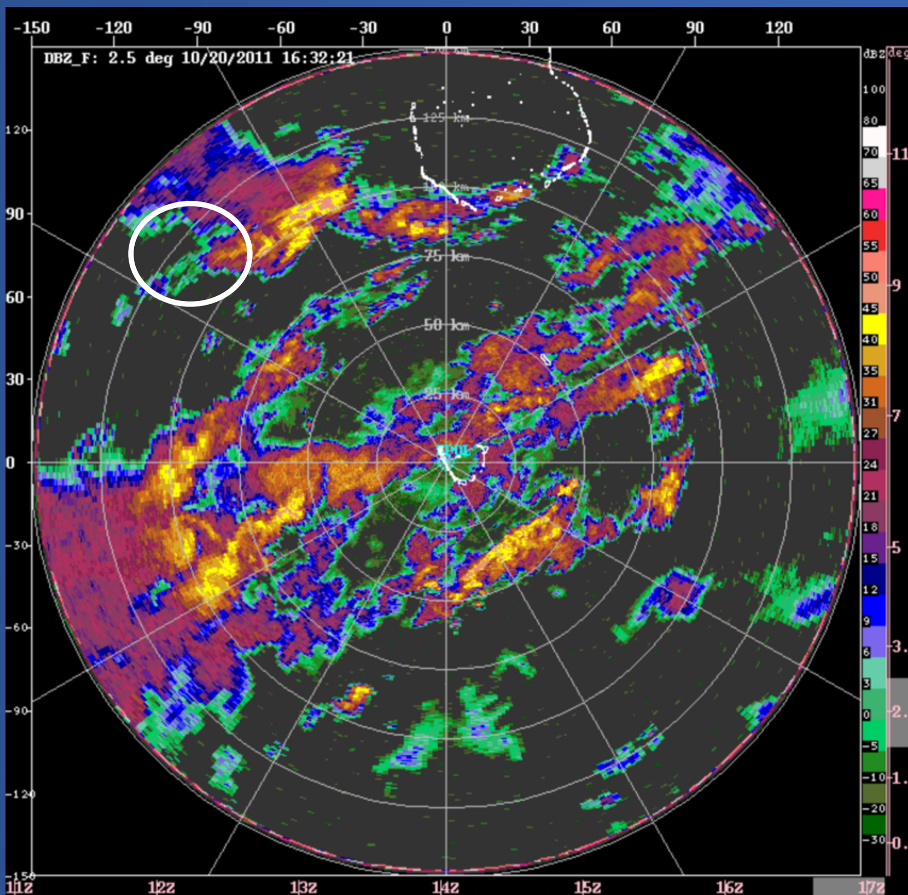

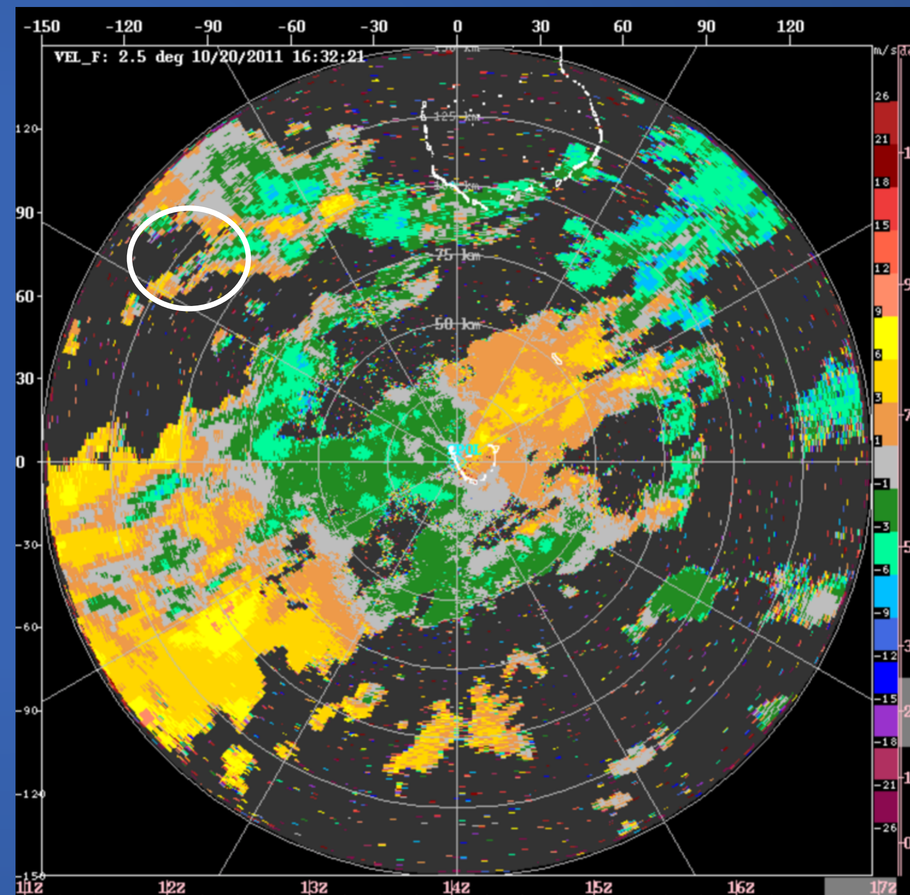

Divergence, vorticity and surface fluxes from ASCAT and MERRA

20 October 2011 16:54:21 UTC

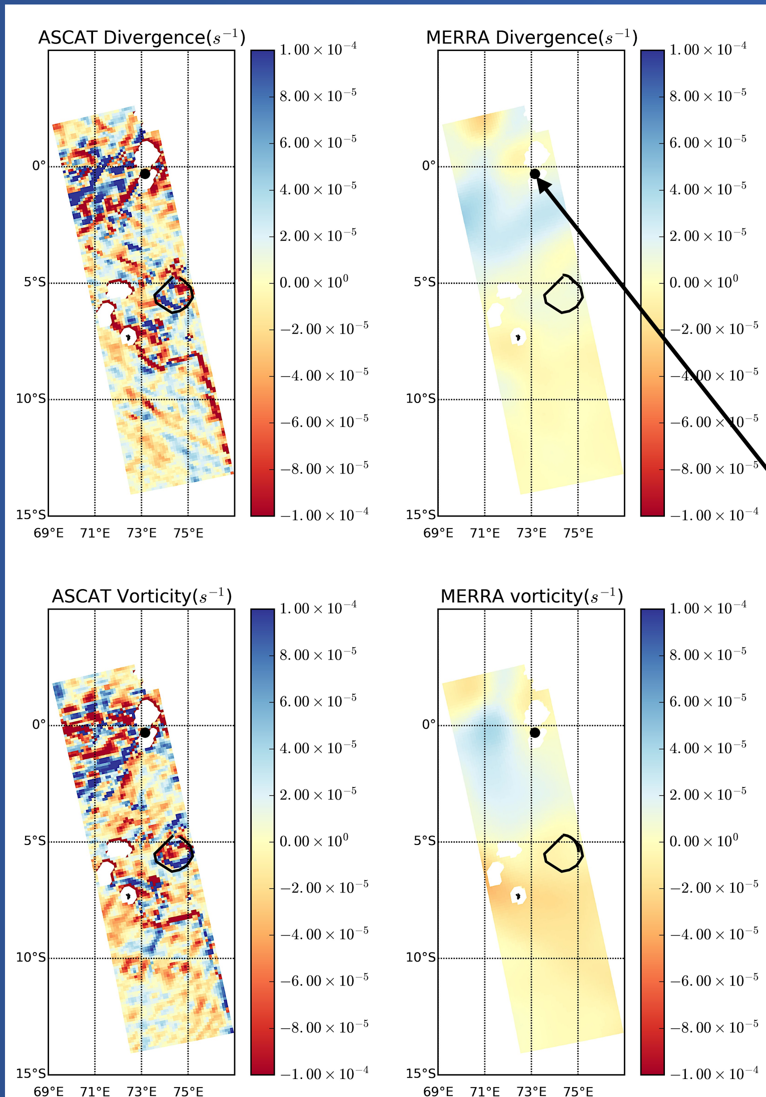

Addu Atoll,
S-PolKa

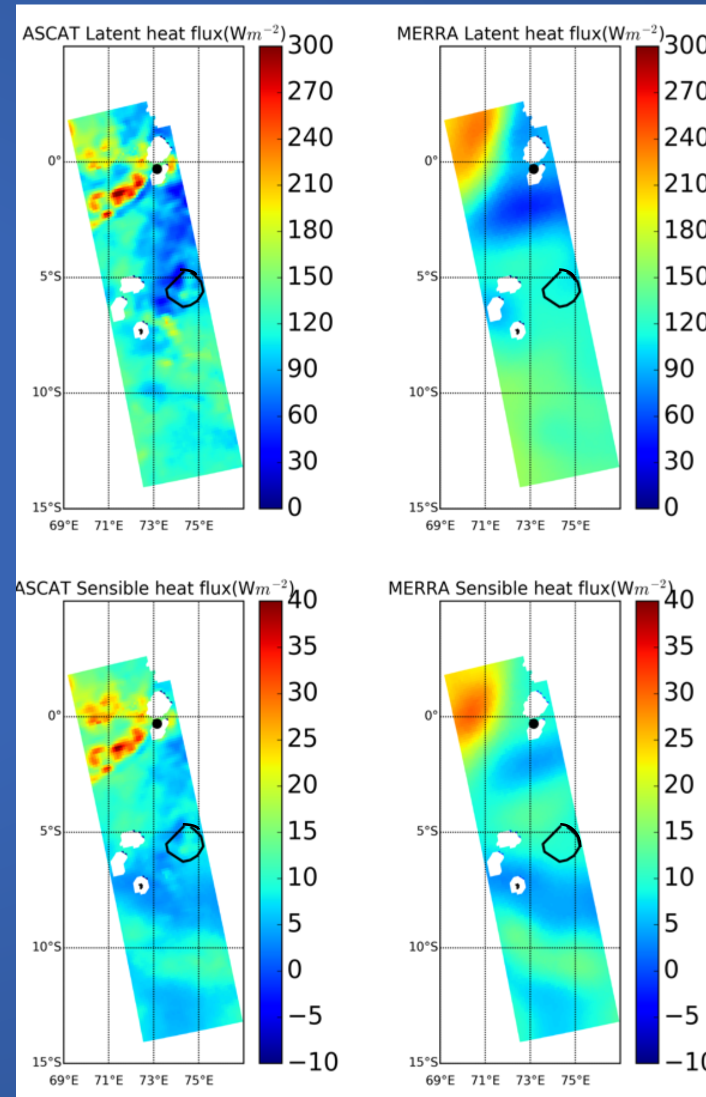

Divergence, vorticity, T_v and OLR for WRF Simulation with ASCAT GF overlaid

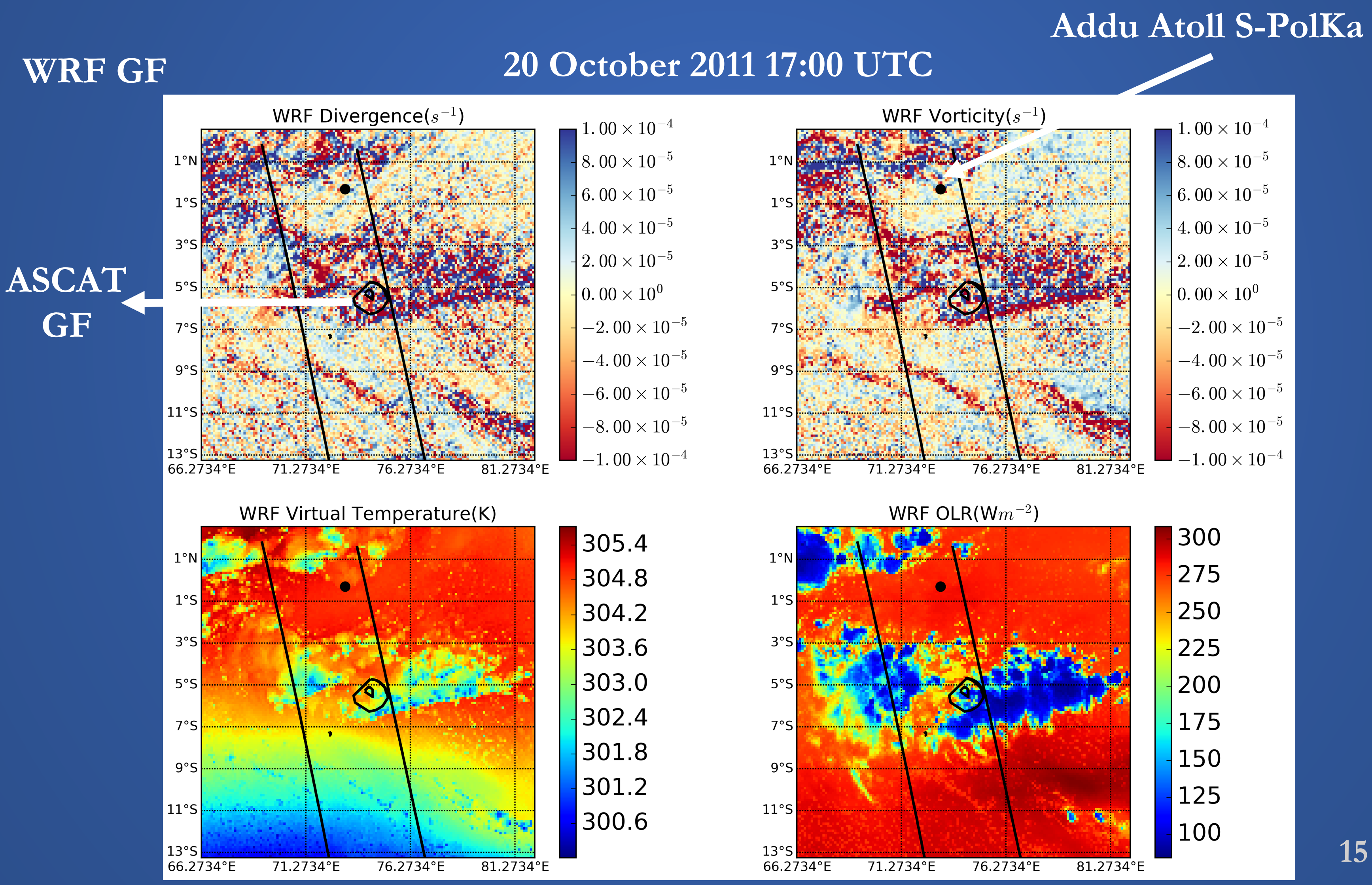

Virtual Temperature (K) with ASCAT swath overlaid

WRF GFs
20 October 1700 UTC

Solid Line – ASCAT GF
Dashed line – WRF GFs

Addu Atoll,
S- PolKa

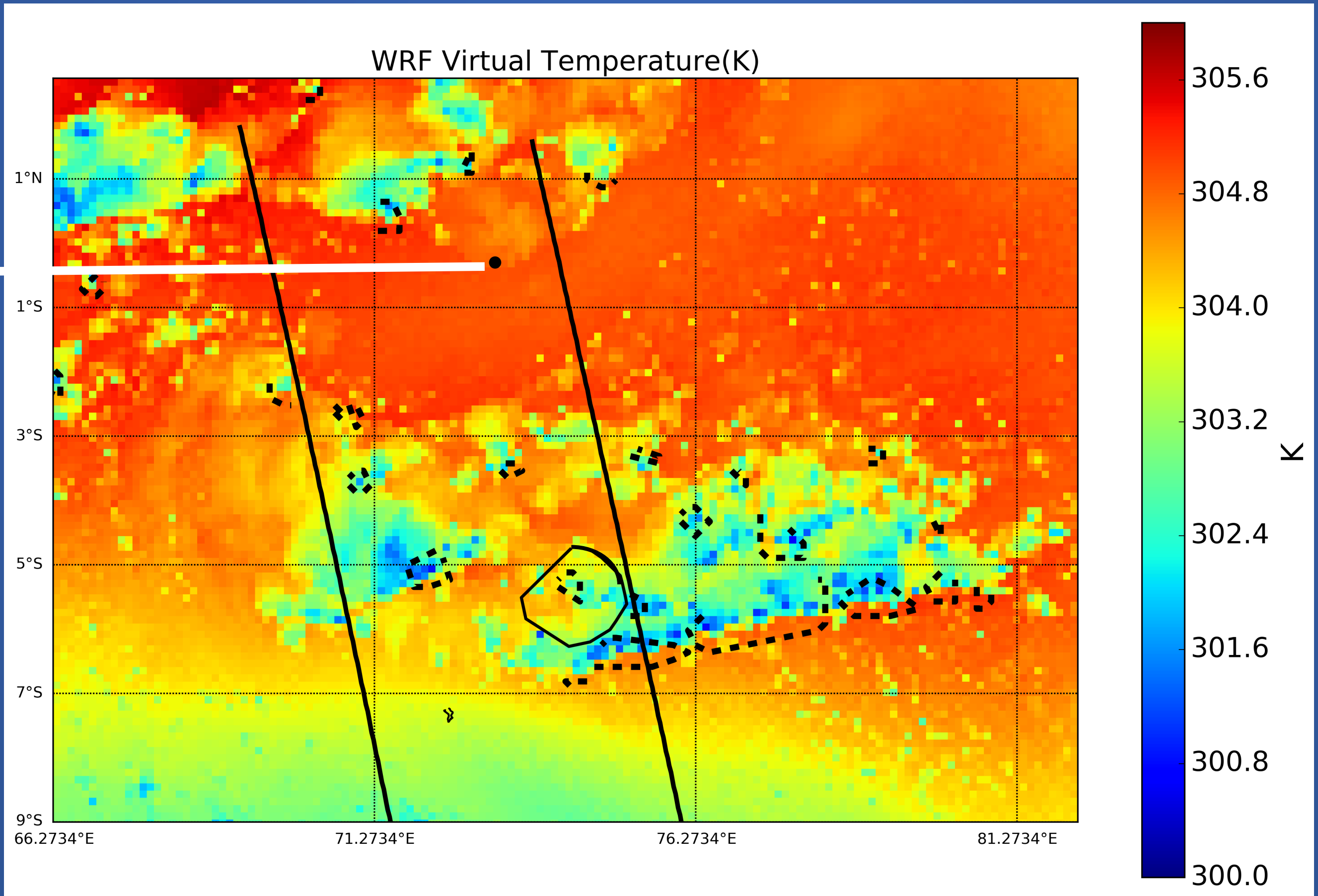

Virtual Temperature (K) with ASCAT swath overlaid

WRF GFs

20 October 2011 1730 UTC

Solid Line – ASCAT GF
Dashed line – WRF GFs

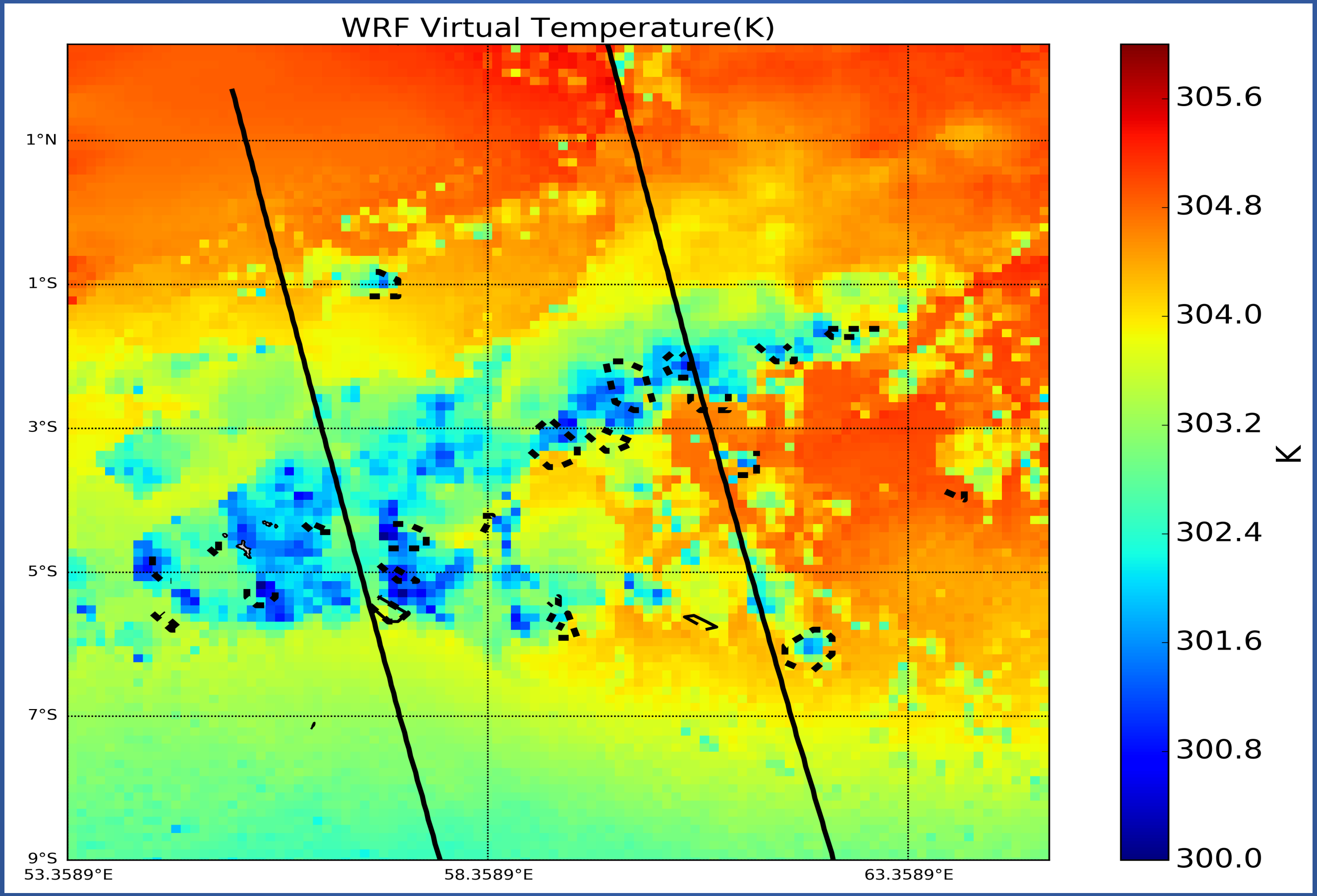

Frequency of GFs over WRF domain for 19-20 October 2011

ASCAT

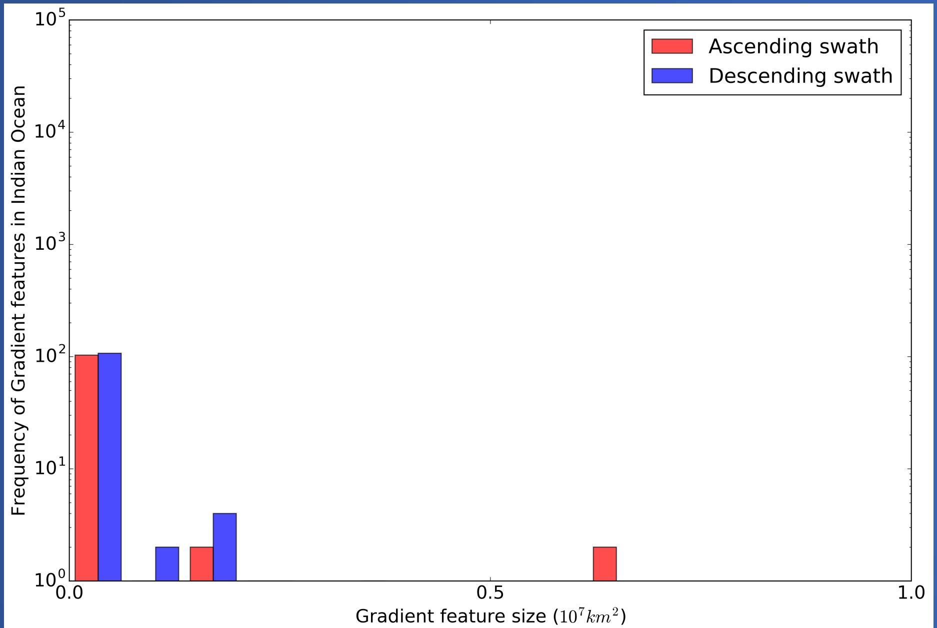

WRF

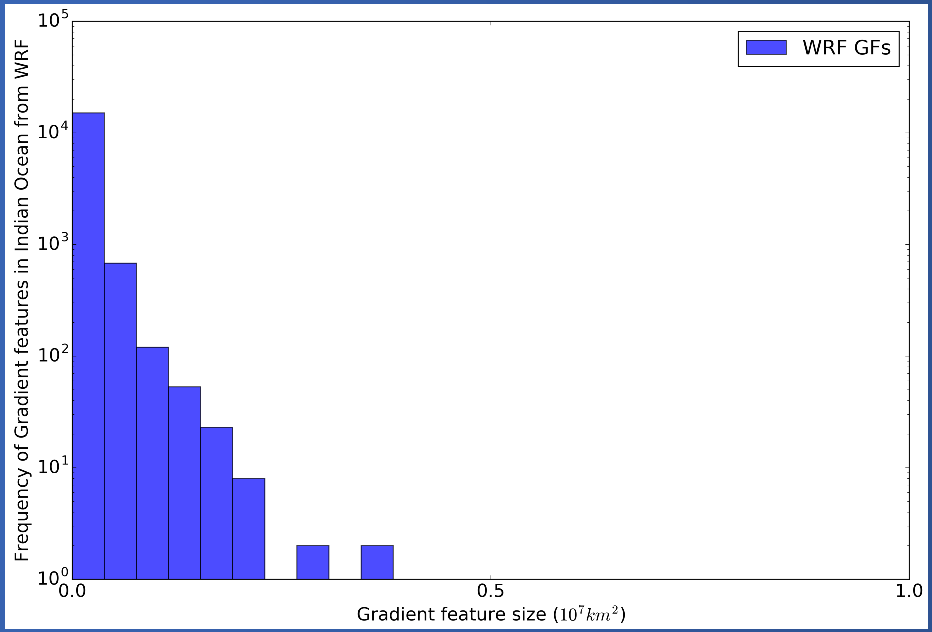

- WRF is producing smaller and a larger number of cold pools as compared to ASCAT for the above period

Global ASCAT-A Climatology Results

Density of GFs (20 million) in a 0.5^{o} grid box for 2007-2015

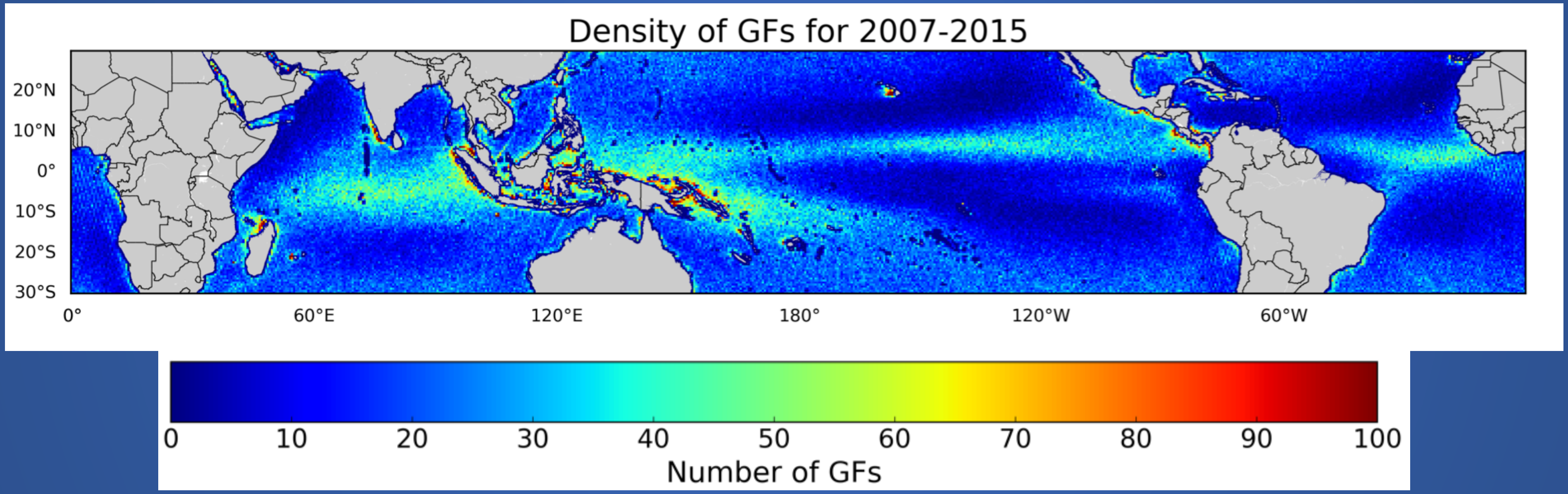

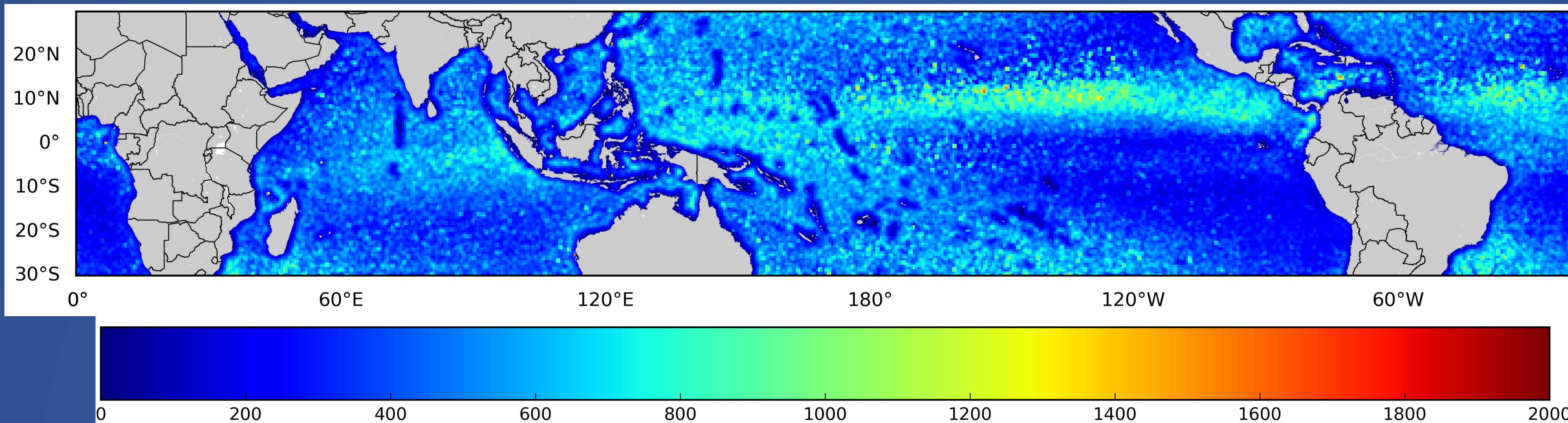

Distribution of GFs according to number of pixels in a 0.5^o gridbox

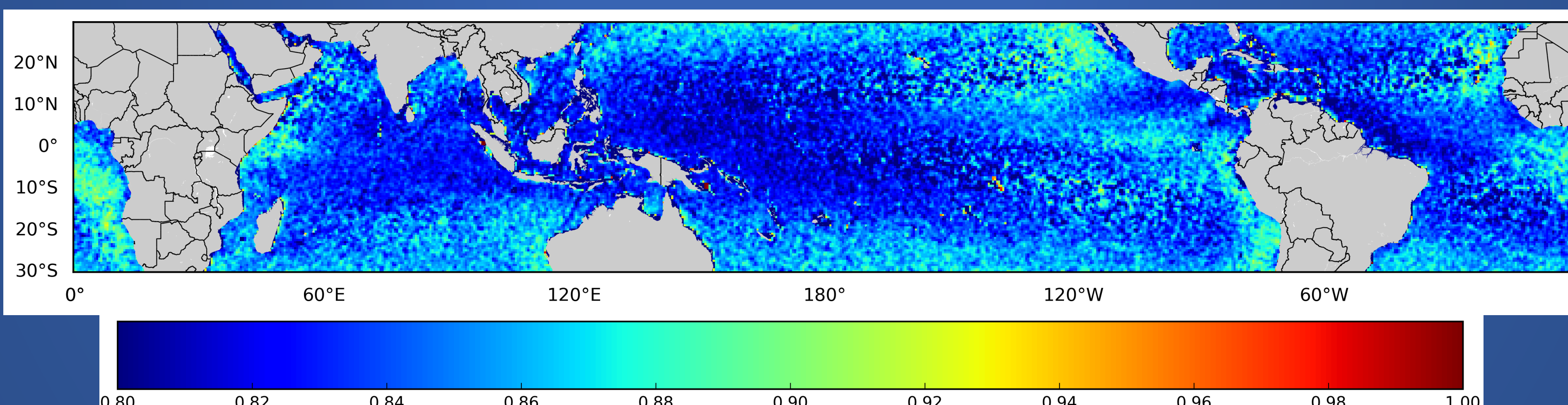

Distribution of GFs according to eccentricity in a 0.5^o gridbox

Global frequency of GFs based on their sizes

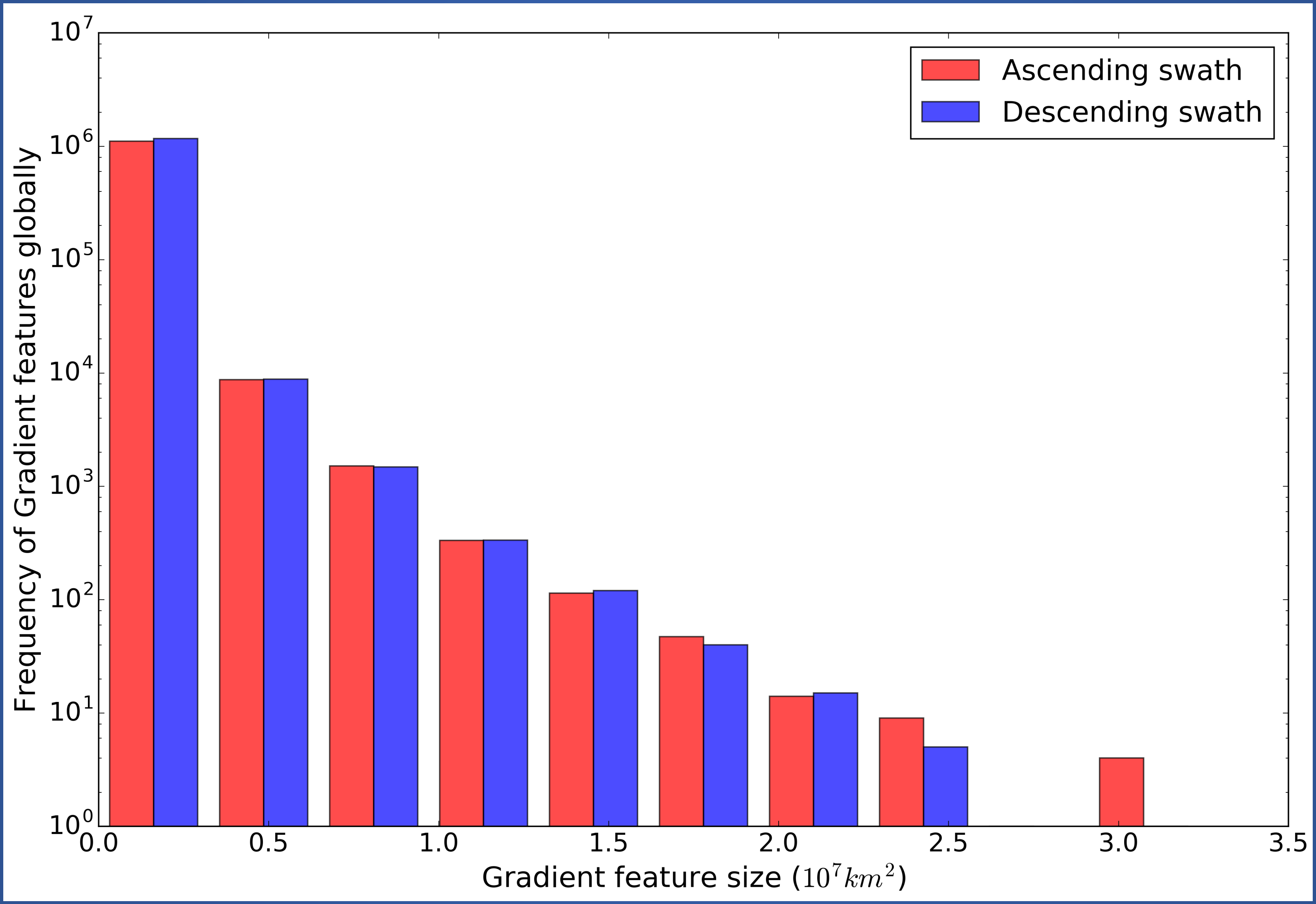

Conclusions

- The locations of low virtual temperature (T_v) and WRF-GFs agree well in WRF, suggesting that these features are cold pools.
- WRF does not reproduce the pattern of observed cold pools, but we do not expect the model to be able to reproduce the observed structure of tropical convection in such a weakly-forced environment
- Regridded WRF in this comparison created smaller cold pools overall, as compared to the climatological distribution of GFs, which may be due to retrieval uncertainty (noise), or the fact that the model produces too many cold pools.

Conclusions (continued)

- For 2007-2015, global density of GFs match well with the precipitation pattern over the tropical oceans, which gives us confidence along with our WRF tests that our approach finds gradient features associated with precipitation processes.

- Surface sensible and latent heat fluxes calculated using ASCAT winds produce much more variability compared to MERRA-2 inherent fluxes.

Future Work

- Working on a python based tool to match the radar and ASCAT swath for DYNAMO, so as to create a better picture of convection in the region.
- Running WRF in the DYNAMO case with ECMWF initial conditions and comparing the results with the current simulation.
- Make other comparisons of GFs with near-coastal radars elsewhere (Kwajalein, Guam)
- Examine regional and seasonal variations in global GF properties identified from scatterometer winds.

Acknowledgements

- NASA OVWST grant.
- Stampede XSEDE
- Remote sensing systems